

ArchNURBS: a NURBS-based tool for the safety assessment of masonry arched structures in MATLAB

Andrea Chiozzi^{a,*}, Marcello Malagù^{a,b}, Antonio Tralli^a, Antonio Cazzani^c

^aUniversity of Ferrara, DI — Dept. of Engineering, via Saragat, I-44100 Ferrara, Italy

^bDelft University of Technology, Faculty of Civil Engineering and Geosciences, Stevinweg 1, 2628 CN, Delft, The Netherlands

^cUniversity of Cagliari, DICAAR — Dept. of Civil and Environmental Engineering and Architecture, 2, via Marengo, I-09123 Cagliari, Italy

Abstract

A new approach towards a fully CAD-integrated structural analysis of masonry arch structures is proposed. It is addressed to professionals dealing with restoration or structural rehabilitation of historical constructions. By using it, they can easily produce estimates of the carrying capacity of curved members, especially, but not exclusively, arches of arbitrary shape. A CAD (Computer Aided Design) environment, which is widely popular among professionals, is employed to provide a NURBS (i.e. Non-Uniform Rational B-Splines) representation of the arch geometry. On the basis of such a representation it is then possible performing both an isogeometric finite element elastic analysis and a limit analysis of the structure up to the collapse load. In this way the load bearing capacity of the arch may be assessed. Moreover, the developed method is also devised for handling the presence of FRP (Fiber-Reinforced Polymers) reinforcement strips at the extrados and/or the intrados. This allows for the design of properly dimensioned reinforcement and its verification according to recently developed building codes. The entire procedure relies upon a sound theoretical background. This approach leads to the development of a practical computational tool for the analysis of masonry arches, which is based on a combination of Isogeometric Analysis and of a suitable implementation of the *Safe theorem* originally proposed by Heyman. The proposed tool has finally been implemented into a MATLAB[®]-based code named ArchNURBS which is going to be distributed as an open-source software.

Keywords: masonry arches, NURBS, isogeometric analysis, limit analysis, FRP reinforcement

1. Introduction

The paper is concerned with an ancient topic, the analysis of the structural behavior of curved masonry members like arches, which is here being revisited through modern tools leading to the implementation and development of a new MATLAB[®]-based open-source computational tool named ArchNURBS.

Currently, there is a large amount of literature regarding the analysis up to collapse of masonry arches and several methods are available for the assessment of the mechanical behaviour of historical masonry constructions and we

*Corresponding author. Tel: +39-0532-974822.

Email addresses: chzndr@unife.it (Andrea Chiozzi), mlgmcl@unife.it (Marcello Malagù), tra@unife.it (Antonio Tralli), antonio.cazzani@unica.it (Antonio Cazzani)

refer to [1] and [2] for an extensive state-of-the-art survey. A number of pieces of commercial softwares which allow
30 evaluating the bearing capacity of a masonry arch have been developed [3, 4, 5]. However, these softwares mainly
cover those cases in which the arch shape is a polyline. Nonetheless, even though many arches may be correctly
represented by a polyline, there is a wide class of arches which are not. For instance, as shown in Figure xx, this is
the case of either rounded stone voussoirs arches or masonry arches in which the dimensions of the blocks are much
smaller than the arch characteristic dimensions (i.e. span and midspan rise). Furthermore, a suitable approach capable
35 of accurately and efficiently analyzing these cases is still lacking. Computer Aided Design (CAD) may be a natural
environment in which to develop a tool for the analysis of such arches which is both efficient and readily usable for
professionals in the field of structural engineering and structural rehabilitation of historical masonry constructions,
among which CAD design representation techniques are currently widespread.

The main reason which makes CAD representation particularly suitable for a subsequent integrated structural
40 analysis of curved masonry members lies in the fact that CAD representation of an arch of arbitrary shape is obtained
through the use of Non-Uniform Rational B-Splines (NURBS). NURBS consist of polynomials which match each
other smoothly (i.e. they are continuous with their derivatives up to a certain order) in such a way that a given set of
points lying in a known range are suitably approximated with a sufficiently high degree of regularity. Development of
NURBS began in the 1950s and was carried out by engineers who needed a mathematically precise representation of
45 freeform surfaces like those used for ship hulls, aerospace exterior surfaces, and car bodies, which could be exactly
reproduced whenever it was technically needed. NURBS are commonly used in Computer-Aided Design (CAD),
Manufacturing (CAM), and Engineering (CAE) systems and are part of numerous industry-wide standards. They
can be efficiently handled by the computer programs and yet allow for easy human interaction. In general, editing
NURBS geometries is highly intuitive and predictable. Moreover, NURBS exactly represent particular geometries
50 such as circles, parabolas and ellipses [6].

In the last decade, NURBS have been extensively studied and developed for both describing the geometry of a
structural model and for representing (in the role of basis functions) the displacement field within the Finite Element
Method (FEM) [7]. Even if the use of polynomial functions belonging to the spline family for the approximate
solution of boundary value problems dates back almost four decades (see e.g. [8, 9, 10, 11]) this new method, which
55 is known as Isogeometric Analysis (IGA), was precisely developed to cover the wide existing gap between the worlds
of FEM and CAD (see e.g. [7, 12, 13, 14, 15]). As it is well-known, the term *isogeometric* is referred to a coincidence
of the geometric model, which is built in a CAD environment, and the structural model (i.e. FEM model) used for
performing stress analysis. In traditional FEM analysis structural model and geometric model never coincide since
they are both representations of a true object but relying on different basis functions. This, in turn, produces accuracy-
60 related issues in the computations, particularly for curved thin structures like arches. Besides, if NURBS are used
as basis functions, their smoothness is inherited by the FEM model, too: this is particularly important because it
allows circumventing some serious difficulties in developing finite elements, e.g. flexible beams and plates where
both bending and shear deformation must be accounted for. Moreover, the better a function is approximated, the

smaller the error affecting its derivatives: since stress fields are not the primary solution variables, but need to be
65 computed by differentiating displacements through post-processing techniques, smoother displacement fields ensure
a more accurate approximation of the stresses.

On the other side, the growing interest in the preservation of masonry structures gave, in the past, an impulse
towards the development of new efficient tools for evaluating the ultimate load-bearing capacity of these structures,
and in particular of masonry arches. From a mechanical point of view, the analysis of masonry arches begins with the
70 contributions of the late 1600s English school (Hooke, Gregory) who stated the analogy between the inverted shape
of a catenary and a compressed arch. Nowadays a sound theoretical framework for the evaluation of masonry arches
exists and it can be affirmed (following Huerta [16] and Como [17]) that the modern theory of limit analysis of masonry
structures, which has been developed mainly by Heyman [18, 19], is a powerful tool for properly understanding and
analyzing masonry curved structures. For the sake of completeness, also the previous papers of Pippard [20] on the
75 analysis of masonry arch bridges and by Kooharian [21] (whose seminal idea appeared in his Ph.D. thesis at the
Brown University in 1952) must be cited. Many other methods of analysis, other than limit analysis, can be used, of
course, for determining the ultimate load carrying capacity of masonry arch bridges, e.g. non-linear FEM analysis,
discrete element analysis, hybrid discrete/finite element methods etc. (see, for instance, [22, 23, 24]) and a number
of commercial FEM codes have been developed (e.g. DIANA). However, with such methods the collapse load is
80 identified as a by-product of an indirect and potentially long iterative non linear analysis procedure, which is often
prone to numerical instabilities. Moreover, a non-linear incremental analysis of a masonry structure requires the
definition of many material parameters which have to be precisely known in order to get reliable results. Finally, limit
analysis may simply be extended to the case of masonry having a limited compressive strength (see e.g. [25, 26]) and
to the case of FRP (fiber-reinforced polymers) reinforced arches (see e.g. [27, 28, 29]).

85 In this paper, a new open-source CAD-based tool for the analysis of masonry arches which is specifically addressed
to professionals in the field of structural engineering and structural rehabilitation of historical masonry constructions
is proposed. The tool, named ArchNURBS and developed in MATLAB[®] environment, is based on a combination of
IGA and limit analysis, both relying on the NURBS representation of the arch which can be easily obtained from
CAD design softwares which are very popular among professional architects and civil engineers. For the reasons
90 discussed previously, NURBS representation of the arch guarantees the highest accuracy of the analyses, especially
when compared to a standard polyline representation of the same arch. IGA is used in order to allow for a finite-
element elastic analysis of the arch which can be useful to assess the response of the arch under usual service loads
which might not drive the thrust line out of the shape of the arch. It is here to be noticed that even if standard curved
finite elements could be used to accurately analyze an arch of arbitrary shape, these instruments are quiet advanced
95 and often out-of-reach for a professional engineer or architect whereas IGA allows for greater accuracy without any
particular additional effort for the final user. On the other hand, limit analysis, for which an equilibrium formulation
is chosen, is used in order to assess the ultimate bearing capacity of the arch. Therefore, the tool allows for a fast
evaluation of the mechanical response of a masonry arch under various loading conditions. Furthermore, algorithms

which allows to take into account the effect of masonry crushing and of additional FRP reinforcements placed at the intrados or extrados of the arch have been devised and implemented.

The need for such a tool is particularly felt, especially if one considers the widespread damages that the 2012 Emilia earthquake produced to ancient historical buildings, with a great loss for Italian cultural heritage; after the earthquake professionals engineers and architects have been called to assess the safety of very many ancient masonry constructions, in which arched and vaulted systems are recurrent, and to devise effective seismic retrofit interventions. An other reason lies in the fact that since the exact shape of the arch to be studied is usually not known in advance, a precise surveying of the structure is needed. This surveying is very often carried out through the use of laser scanning techniques which may be imported in a CAD environment as a cloud of points. A CAD exact representation of the arch geometry is then possible and constitutes the basis upon which both the elastic and limit analysis can be performed in an integrated way, by exploiting new computational mechanics tools, in particular IGA [7]. It should be noticed that surveying gives the actual arch configuration, which usually already exhibits elastic deformations (which are generally neglectable) and inelastic settlement of the arch springers.

ArchNURBS is thus the first computational tool which, exploiting the procedures above mentioned, allows for the evaluation of the load bearing capacity of arch structures arbitrarily loaded, starting from a NURBS representation of the topographical survey of the real arch obtained in a CAD design environment.

The paper is organized as follows: in Section 2 a synthetic survey on NURBS description of the shape of masonry arch is provided. The adopted structural models and isogeometric elastic analysis are recalled and commented upon in Section 3. The limit analysis based on the NURBS geometry representation and its application to FRP reinforced arches and to masonry arches having a limited compressive strength will be addressed in Section 4. Section 5 is devoted to presenting some meaningful numerical examples developed within ArchNURBS. Finally, conclusions and suggestions for future developments will be put forth in Section 6.

2. Geometry description

Description and computation of geometries in commercial CAD packages are based on B-splines and NURBS. More precisely, NURBS basis functions are built on B-splines basis functions which are piecewise polynomial functions defined by a sequence of coordinates $\Xi = \{\xi_1, \xi_2, \dots, \xi_{n+p+1}\}$, which is known as the *knot vector*, in which the so-called *knots* $\xi_i \in [0, 1]$ are points in a parametric domain whereas p and n denote the order and the number of the basis functions, respectively. The distance between two consecutive knots is named knot span and it represents the equivalent of the element domain for traditional finite elements. Once the order of the basis functions and the knot vector are known, the i -th B-spline basis function $N_{i,p}$ can be computed by means of the Cox-de Boor recursion formula [30, 9], which is not reported here for the sake of brevity.

As previously mentioned, B-splines are the starting point for the computation of the NURBS basis functions.

Indeed, given a set of weights $w_i \in \mathbb{R}$, the NURBS basis functions $R_{i,p}$ read

$$R_{i,p}(\xi) = \frac{N_{i,p}(\xi) w_i}{\sum_{i=1}^n N_{i,p}(\xi) w_i}. \quad (1)$$

NURBS share many properties with B-spline basis functions [6]. Among these, they are both non-negative, they have a compact support and build a partition of unity (PoU), that is

$$\sum_{i=1}^n N_{i,p}(\xi) = \sum_{i=1}^n R_{i,p}(\xi) = 1 \quad (2)$$

for each $\xi \in [0, 1]$ (see [7]). Hence, it is noteworthy from (1) and (2) that B-spline basis functions are NURBS basis functions with weights w_i are all equal to 1. However, NURBS basis functions have the great advantage of representing exactly the geometry of a wide set of curves such as circles, ellipses and parabolas [6] and of the surfaces generated by them.

B-spline and NURBS geometries are computed as linear combinations of basis functions [6, 31]. For instance, if we consider a set of B-spline basis functions $N_{i,p}$ (the same holds for the NURBS basis functions) with $i = 1, \dots, n$, we define the curve $\mathbf{C}(\xi) \in \mathbb{R}^d$ as

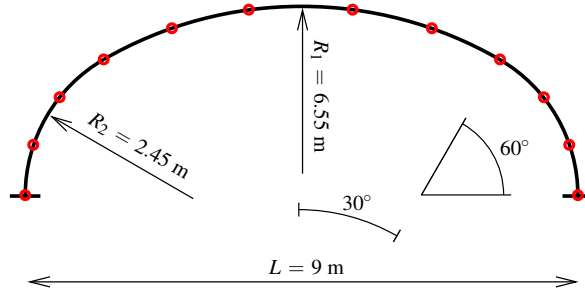
$$\mathbf{C}(\xi) = \sum_{i=1}^n N_{i,p}(\xi) \mathbf{B}_i, \quad (3)$$

where the coefficients $\mathbf{B}_i \in \mathbb{R}^d$ are known as control points (in the following, we assume $d = 2$ since this work focus on planar curves). Differently from standard Lagrange and Hermite approximations, B-spline geometries do not usually interpolate these points. The continuity of the curve follows from that of the adopted basis functions [7] that, in general, is \mathcal{C}^{p-1} throughout the domain. However, if a knot has multiplicity m , the continuity decreases m times at that point (see [6]).

Modeling CAD geometries inevitably involves several ingredients, such as knots, order of the approximation and control points. However, in many practical applications only few of these parameter are known *a priori*. In reverse engineering processes, for example, CAD models are created by interpolating or approximating a set of points $\mathbf{P}_i \in \mathbb{R}^2$ usually obtained from the real object by means of laser scanners. Nonetheless, the parameterization of the input data for B-spline and NURBS geometries addresses a crucial issue concerning the fairness of the final curve. Hence, there have been several attempts to improve the accuracy of B-spline and NURBS approximations and interpolations [9, 32, 33, 34, 31]. In particular, some of these parameterization techniques, such as the uniform method, the arch-length method and the centripetal method are available in several CAD softwares [35].

The easiest way to assess the quality of the computed curve is to evaluate the distance between the CAD geometry $\mathbf{C}(\xi)$ and the analytical representation of the real curve $\mathbf{F}(\xi)$. Therefore, the distance between these two curves at the parametric point ξ is calculated as

$$d(\xi) = \min_{\xi} \{ |\mathbf{C}(t) - \mathbf{F}(\xi)| \}. \quad (4)$$

Figure 1: Polycentric arch (red circles denote the interpolating points \mathbf{P}_i)

n^0 of \mathbf{P}_i	10	20	40
E_∞ [m]	1.34e-2	0.79e-2	0.39e-2
E_2 [m]	1.64e-3	3.73e-4	2.74e-5

Table 1: Maximum and mean errors on the approximation of the polycentric arch.

Once the value of $d(\xi)$ has been evaluated for n given data points, we define the errors in the L_∞ norm:

$$E_\infty = \max_{i=1}^n \{d_n\}, \quad (5)$$

and in the L_2 norm:

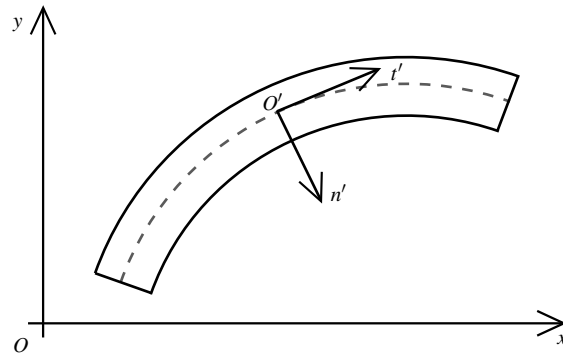
$$E_2 = \left[\frac{1}{n} \sum_{i=1}^n d_n^2 \right]^{1/2}. \quad (6)$$

Thus, for the sake of completeness we investigate the quality of the NURBS curve in Figure 1 in approximating of a polycentric arch composed of three circular arcs jointed together with \mathcal{C}^1 continuity. The radius R_i and the center of each portion are also shown. The NURBS curve has been drawn in AutoCAD[®] 2013 by interpolating the set of points \mathbf{P}_i indicated by red circles in Figure 1 with cubic NURBS basis functions. In particular, the position of these points has been calculated by dividing each of the three circular arcs in equal parts. As it is shown in Table 1, both the maximum (i.e. E_∞) and the mean (E_2) errors between NURBS approximations and the polycentric arch decreases with the number of interpolating points as it is expected.

3. Linear elastic analysis

In this Section we introduce the Isogeometric Analysis of curved Timoshenko beams [36]. Interesting studies on Isogeometric Analysis of curved rods (even though Kirchhoff-Love rods) in the three dimensional space may be found in [37, 38].

As it is depicted in Figure 2, we consider a Cartesian reference system $O(x,y)$ and a local reference system $O'(t',n')$ where t' and n' are the tangent and the normal vectors to the beam axis. Further, we introduce the curvilinear abscissa $s \in [0, l]$ which spans the centroidal line of the plane curved beam of length l defined by the parametric

Figure 2: Reference system $O(x,y)$ and local reference system $O'(t',n')$

representation

$$\begin{cases} x(s) = \sum_{i=1}^n N_{i,p}(s(\xi)) x_i & \text{and} \\ y(s) = \sum_{i=1}^n N_{i,p}(s(\xi)) y_i \end{cases} \quad (7)$$

where x_i and y_i are the control points coordinates. Thus, the unit tangent and normal vectors of a NURBS curve at a parametric point s are calculated as [39]

$$t' = \frac{(x_{,s}, y_{,s})}{\sqrt{x_{,s}^2 + y_{,s}^2}} \quad (8)$$

and

$$n' = (y_{,s}, -x_{,s}) \cdot \frac{x_{,ss}y_{,s} - x_{,s}y_{,ss}}{(x_{,s}^2 + y_{,s}^2)^2} \quad (9)$$

where comma denotes differentiation. Further, the curvature radius reads

$$R(s) = \frac{(x_{,s}^2 + y_{,s}^2)^{3/2}}{|x_{,s}y_{,ss} - x_{,ss}y_{,s}|}. \quad (10)$$

In order to describe the kinematics of a curved Timoshenko beam we consider the displacement and the load vectors

$$\mathbf{u} = [u, v, \phi]^T \quad \text{and} \quad \mathbf{p} = [q_t, q_r, m]^T, \quad (11)$$

referred to the local reference system (where $(\cdot)^T$ denotes the transpose). In particular, u and v are the tangential and normal displacement of the cross-section centroid, ϕ the cross-section rotation, q_t and q_r the tangential and radial distributed loads and m the distributed bending couples. Hence, by assuming small deformations, the equilibrium, compatibility and constitutive equations for the plane-curved Timoshenko beam are

$$N_{,s} - \frac{T}{R} + q_t = 0, \quad T_{,s} + \frac{N}{R} + q_r = 0 \quad \text{and} \quad M_{,s} - T + m = 0, \quad (12)$$

$$\varepsilon = u_{,s} - \frac{v}{R}, \quad \gamma = v_{,s} + \frac{u}{R} + \phi \quad \text{and} \quad \chi = \phi_{,s}, \quad (13)$$

$$N = EA\varepsilon, \quad T = GAk_s\gamma \quad \text{and} \quad M = EJ\chi, \quad (14)$$

where the generalized stresses N , T and M denote the axial force, the shear force and the bending moment, whereas the generalized strains ε , γ and χ are the axial, the shear and the curvature deformations. Finally, the constants E , G , A , J and k_s indicate the Young's modulus, the shear modulus, the cross sectional area, the area moment of inertia and the shear-correction factor.

The first step towards the finite element solution of the problem is represented by the definition of the total potential energy of the system

$$\Pi = \frac{1}{2} \int_0^l (EA\varepsilon^2 + GAk_s\gamma^2 + EJ\chi^2) ds - \int_0^l (q_t u + q_r v + m\phi) ds. \quad (15)$$

Subsequently, by making use of the iso-parametric formulation, the discrete displacement field $\mathbf{u}^h(\xi) \in \mathbb{R}^2$ is defined as

$$\mathbf{u}^h(\xi) = \sum_{i=1}^n N_{i,p}(\xi) \mathbf{u}_i, \quad (16)$$

where $\mathbf{u}_i = [u_i, v_i, \phi_i]$ are the displacements at the control points \mathbf{B}_i . It is worth noticing that, according to eq. (3), the displacement field in (16) has been discretized with B-spline basis functions. Nonetheless, NURBS basis functions might have been used in cases where a NURBS-described curve is given. Hence, by making use of eqs. (15) and (16) the discrete solution of the problem is defined as:

$$\arg \min_{u, v, \phi} \left\{ \sum_{e=1}^{n_e} \left[\frac{1}{2} \int_{\xi_e}^{\xi_{e+1}} \left[EA (\varepsilon^h)^2 + GAk_s (\gamma^h)^2 + EJ (\chi^h)^2 \right] ds - \int_{\xi_e}^{\xi_{e+1}} \mathbf{p}^T \mathbf{u}^h ds \right] \right\}, \quad (17)$$

where n_e is the number of spans whereas ξ_e and ξ_{e+1} are the knots which correspond to the e -th span. Once the numerical solution \mathbf{u}^h is known, the generalized stresses and strains are calculated by means of eq. (13) and (14). Therefore, N , T and M and ε , γ and χ are defined with the same NURBS basis functions used for the approximation of the displacement field \mathbf{u}^h . Accordingly, the computation of the thrust line, which descends from the ratio M/N , is straightforward.

As in standard finite element discretizations, the numerical solution can be improved by refining the approximation. In particular, in IGA there are three different refinement techniques. The first two are knot insertion (h -refinement) and order elevation (p -refinement) which do not alter the geometry and the continuity of the curve. The third method, which is known as k -refinement, consists in order elevation of the basis functions and consequent knots insertion. This increases the continuity of the approximation without changing the geometry [7, 40]. In the developed

program each of these methods may be used.

200 4. Limit analysis

It is well established that when *mechanism* and *equilibrium* formulations of limit analysis are linearized, they produce dual Linear Programming (LP) problems [41]. In particular Livesley [42] has shown that the *equilibrium* formulation can be applied to masonry arches. involve the discretization of the arch into a number of rigid blocks. Many researchers have developed procedures to model masonry arches as discrete rigid blocks: among them we recall [43, 44, 45].

In this paper a joint equilibrium formulation, similar to that originally adopted by Livesley [42] and then proposed for masonry arches in [46] is used. Let us incidentally observe that, while an equilibrium formulation has been formally used, assuming a finite number of blocks (and hence of interfaces) provides actually an upper bound estimate to the collapse multiplier.

210 The adopted model relies on the following traditional assumptions, originally proposed by Heyman (see [47]) for the limit analysis of masonry arches:

- (i) sliding failure of adjacent units in the arch cannot occur;
- (ii) masonry has zero tensile strength;
- (iii) masonry has infinite compressive strength.

215 Therefore, a procedure based on an *equilibrium formulation* and the above assumptions for the limit analysis of masonry arches is set out as follows.

The structure is divided into c elements (blocks) in much the same way as for elastic analysis. Subsequently to this subdivision, $d = c + 1$ interfaces are generated. For each block the equations of equilibrium are written, in such a way as to express contact forces $\mathbf{q} = [T_i, N_i, M_i]$ (which are respectively the shear force, the axial force and the bending moment) acting on the i -th inter-element boundary and any external load acting on the element \mathbf{f} , which can be either a dead load \mathbf{f}_D or a live load $\lambda \mathbf{f}_L$. Such equations may be expressed as:

$$\mathbf{A}\mathbf{q} - \lambda \mathbf{f}_L = \mathbf{f}_D, \quad (18)$$

where \mathbf{A} is a suitable textcolored($3c \times 3d$) equilibrium matrix containing the direction cosines of the normal versor n^i of the transversal section at each contact. These equations are the equilibrium constraints of the problem.

No-tension yield constraints on \mathbf{q} are then defined:

$$\left. \begin{array}{l} M_i \leq 0.5N_it_i \\ M_i \geq -0.5N_it_i \end{array} \right\} \forall \text{ contact } i = 1, \dots, c. \quad (19)$$

225 where t_i is the depth of the arch section at contact i . Finally the limit analysis problem for proportional loading is now written as *Maximize the load factor λ , subject to the equilibrium constraints (18) and the yield constraints (19)*:

$$\max\{\lambda\}. \quad (20)$$

Using this formulation the LP problem variables are the contact forces $(T_1, N_1, M_1, \dots, T_c, N_c, M_c)$ and the unknown load factor λ . In ArchNURBS the linear programming problem is solved through the MATLAB[®] function `linprog.m` which is part of the MATLAB[®] Optimization Toolbox.

230 The yield constraints expressed in (19) are valid only if the material has an infinitely large compressive strength. If it is assumed, instead, that masonry exhibits a limited (i.e. finite) compressive strength σ_{crush} , and that thrust is transmitted through a rectangular crush block, then, as it is suggested in [48], eq. (19) may be replaced by:

$$\left. \begin{aligned} M_i &\leq N_i \left(0.5t_i - \frac{N_i}{2\sigma_{crush} b} \right) \\ M_i &\geq -N_i \left(0.5t_i - \frac{N_i}{2\sigma_{crush} b} \right) \end{aligned} \right\} \forall \text{ contact } i = 1, \dots, c, \quad (21)$$

235 where σ_{crush} is the masonry compression strength and b is the width of the arch transversal section. However, the constraints in eq. (21) are non-linear. Therefore, in order to continue using a Linear Programming (LP) solver, these constraints need to be approximated as a set of linear constraints (see e.g. [46, 48]). In order to maximize computational efficiency, an iterative solution algorithm which involves only refining the representation of the failure envelope (through linear constraints) where required is used. The algorithm can be summarized as follows.

Step 1. Initially solve the global LP problem with the original linear constraints (19) plus the additional linear constraint $N_i < N_{i,max}$ on each contact i , where $N_{i,max}$ is the maximum centered axial force which the arch section is capable to bear before crushing occurs;

240

Step 2. Substitute N_i from the last solution into the inequality constraints, eqs. (21), for each contact i . If a constraint is violated, calculate the violation factor e_i , i.e.:

$$e_i = \frac{|M_i|}{N_i \left(0.5t_i - \frac{N_i}{2\sigma_{crush} b} \right)}, \quad (22)$$

and store, from the previous solution, the values of axial force corresponding to contacts where violation has occurred. Let's call these values $N_{i,0}$;

245 Step 3. For each contact with $e_i \geq 1.0$ (i.e. such that violation occurs) set an additional linear constraint which is tangential to the original failure envelope described by eqs. (21) at the point corresponding to $N = N_{i,0}$;

Step 4. Solve the new global LP problem;

Step 5. Repeat from step 2 until the maximum value of $e_i < 1 + tlr$ where the tolerance tlr is taken as a suitably small value.

Moreover, if sliding between blocks is to be taken into account, additional sliding yield constraints to the linear programming problem (20) are needed. As suggested in [45], while assuming a simple associative friction model, the following *linear constraints* may be defined:

$$\left. \begin{array}{l} T_i \leq \mu_i N_i \\ T_i \geq -\mu_i N_i \end{array} \right\} \forall \text{ contact } i = 1, \dots, c, \quad (23)$$

where μ_i is a suitable friction coefficient for each contact i . This particular friction model has been chosen for simplicity reasons whereas in literature more advanced models exist which involve non-associative friction laws and the use of non-linear programming methods (see e.g. ...).

For the sake of simplicity, backfill (which is considered as a dead load and thus enters in Eq. (18)) is modeled as an external vertical force acting upon each block, which is given by the weight of the volume of the backfill portion lying above each block and is applied to the center of mass of the same volume. Again, It is necessary to point out that in literature much more sophisticated models for backfill exist, which are capable of taking into account effects like load diffusion and the gradual build-up of passive pressures (see e.g. ...).

Furthermore, it is possible to modify the same analysis in order to take into account the presence of CFRP (Carbon Fiber Reinforced Polymer) reinforcement strips at the intrados and/or extrados of the arch. Many researchers have proposed different solutions to this problem (see, e.g., [27, 28, 29]). In the present paper we deal with the problem by modifying the original equilibrium formulation including two further variables ($F_{i,\text{intrados}}, F_{i,\text{extrados}}$) for each of the CFRP reinforced interfaces. These variables represent the inner force acting within the FRP strip at the interface at the intrados and extrados respectively and enters into the equilibrium constraints (18). The new variables are subjected to the *additional yield constraints*:

$$\left. \begin{array}{l} 0 < F_{i,\text{intrados}} < F_d \\ 0 < F_{i,\text{extrados}} < F_d \end{array} \right\} \forall \text{ reinforced contact } i = 1, \dots, n, \quad (24)$$

where F_d is the design delamination resistance of the CFRP strip which may be evaluated, for example, following prescriptions contained in Chapter 5 of [49].

5. Numerical examples

In this section three numerical examples obtained with the computational tool ArchNURBS are presented. In particular, the influence of the geometric representation of the rigid blocks in which the arch is subdivided on the limit

Mechanical Properties	Example discussed in Section 5.1	Examples discussed in Sections 5.2 and 5.3
Masonry Young's modulus (E)	2800 MPa	1500 MPa
Masonry shear modulus (G)	860 MPa	500 MPa
Masonry mass density (ρ_m)	1800 kg/m ³	1800 kg/m ³
Masonry compressive strength (f_c)	6.0 MPa	2.4 Mpa
Backfill mass density (ρ_b)	1600 kg/m ³	1600 kg/m ³

Table 2: Masonry mechanical properties and backfill density for examples in Sections 5.

load multiplier λ is first discussed. Then, the limit analysis for the three-centered arch described in Section 2 and a *real world* arch are taken into consideration in the second and third example, respectively.

275 5.1. Influence of the voussoirs geometry

Many arches in the real-world occurrences are made of stone voussoirs which generally have a rounded shape rather than a quadrangular shape as shown in Figure 3(a). When the size of these voussoirs is not small their exact geometric representation is of paramount importance in order to obtain accurate estimates of the collapse load multiplier λ .

280 The structural analysis tool proposed in the present work allows for an exact description of the rounded shape of the voussoirs of the arch by exploiting the NURBS features. On the contrary, most of existing commercial software codes approximate the shape of rounded voussoirs with a quadrangular shapes.

Hence, we consider a semi-circular arch with mean radius 2.125 m and section depth 0.250 m and width 0.500 m. The backfill height is assumed equal to 3.00 m and it is loaded with a uniformly distributed vertical live load of
285 1 kN/m. The arch is subdivided into ten voussoirs. Material properties of the stone-voussoirs and of the backfill are reported in Table 2.

In this case a collapse load multiplier $\lambda = 9.8$ is computed for the arch model with rounded voussoirs. The obtained value is the exact collapse load multiplier for the rounded voussoirs arch here described.

290 On the other hand, if the arch is modeled by means of ten quadrangular voussoirs $\lambda = 8.9$. Therefore, the geometrical approximation of the rigid blocks implies an error of 9.2 % on the estimate of λ .

Of course, the error could be greatly reduced if an higher number of quadrangular blocks was chosen to model the arch but then the number of interfaces between blocks (on which hinges positions are constrained to be) would be changed in respect to the original problem. In addition, computational efficiency would be clearly reduced.

295 In Figures 3(b)-(c) a comparison between the two arch models is shown along with a plot of the corresponding thrust line.

5.2. Three-centered arch

The three-centered arch presented in Section 2 is examined. In particular, its depth and width are assumed equal to 0.560 m and 0.500 m, respectively. Material properties used for masonry and for the backfill are reported in

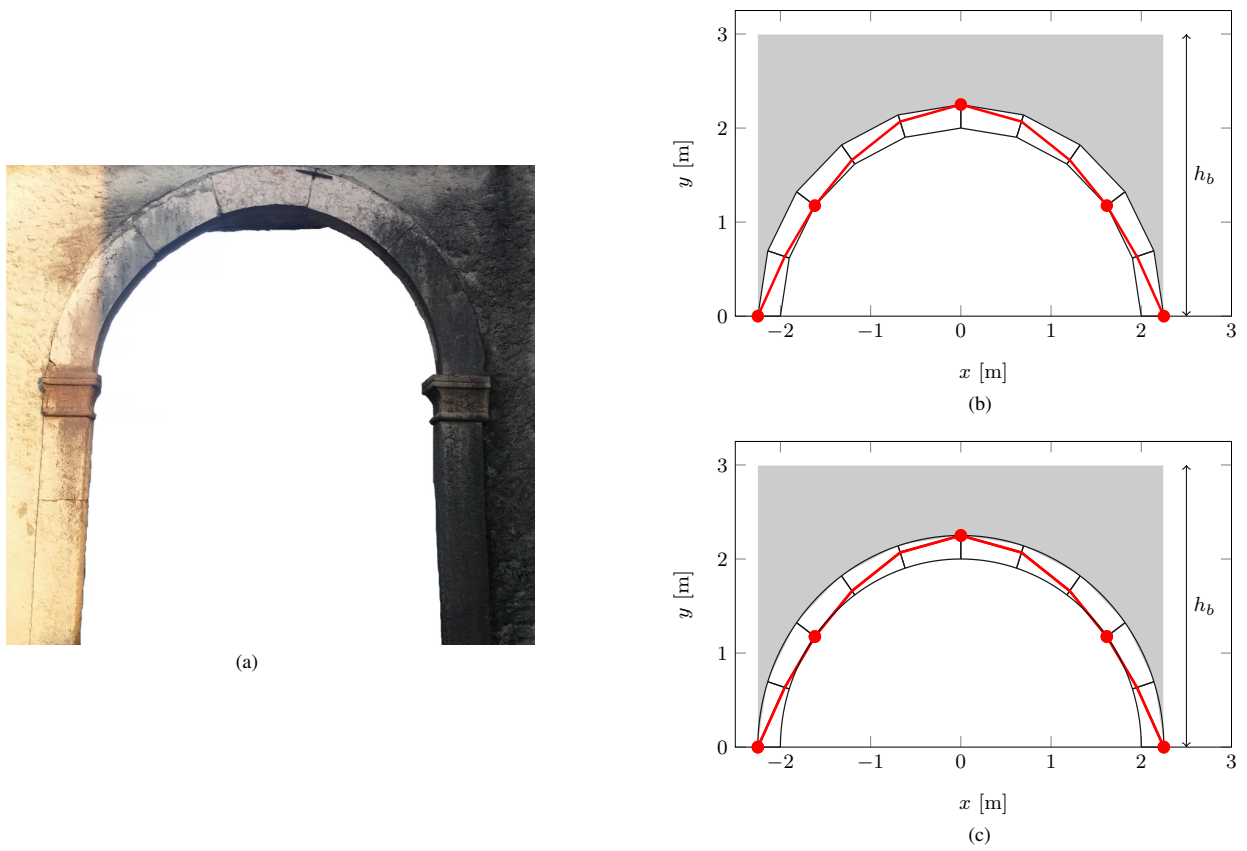


Figure 3: (a) Example of rounded voussoirs arch (Calvene, Italy). Thrust lines computed with (a) quadrangular voussoirs and (b) rounded voussoirs example arch models.

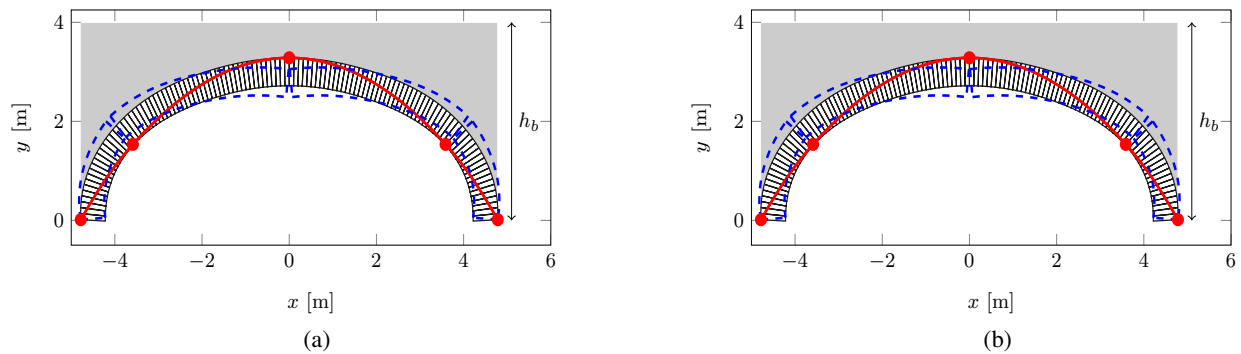


Figure 4: Three-centered arch: thrust line (red solid line) obtained without backfill (a) and with backfill (b). The collapse load multipliers corresponding to these configurations are 1.42 and 28.26, respectively.

Table 2. The masonry mechanical properties chosen are typical for low quality masonry as suggested in the explicative circular [50] related to the Italian Building Code [51].

The arch is supposed to be loaded by a downward linear uniform live load of 1 kN/m. This load is amplified by a load multiplier λ . The arch has been subdivided into 90 rigid blocks. First, limit analysis is performed without considering any backfill. In this case the collapse load multiplier is $\lambda = 0.78$. As it is illustrated in Figure 4(a) the resulting collapse mechanism is a symmetrical five hinges mechanism. The corresponding thrust line and position of hinges at collapse is indicated by a red line and red circles, respectively.

The same analysis has been then carried considering a backfill having a height of 4.00 m and a specific weight as indicated in Table 2. In this case, despite the collapse mechanism and the position of the collapse thrust line being similar to those obtained in the previous case, the load multiplier increases to $\lambda = 21.62$. Therefore, the particular geometry of the arch is very sensitive to the stabilizing effect of the backfill.

It is worth noticing that a relatively high collapse load multiplier has been calculated in the last case. Such a value is due to the fact that the shape of the arch nearly contains the funicular for that particular load configuration [19].

5.3. A masonry arch from Torre Fornasini

The third arch here analyzed is a real world masonry arch belonging to the groin vault which bears the first story of *Torre Fornasini*, a historical masonry tower construction in Poggio Renatico (Italy), which was severely damaged by the earthquake which struck Emilia on May 2012. The tower, depicted in Figure 5, has been subjected to extensive seismic retrofit intervention which comprised reinforcement of the extrados of the vault with Carbon Fiber Reinforced Polymers (CFRP) strips [52]. In particular, the analyzed arch is the segmental arch shown in Figure 6(a). It is characterized by a span equal to 4.13 m, a midspan rise equal to 1.81 m, a depth equal to 0.14 m and a width equal to 0.25 m. Again, material properties assumed for masonry and specific weight for the backfill are reported in Table 2. The arch is loaded by a downward acting linear uniform live load equal to 1 kN/m multiplied by a load multiplier λ . The arch has been subdivided into 90 rigid blocks. First, limit analysis is performed without taking into account any backfill. In this case a solution cannot be determined since the arch is not stable under its own weight. Then,

the same analysis is carried out by considering a backfill with specific weight reported in Table 2 and a maximum height equal to 2.15 m. Under these assumptions, the optimization problem can be solved and the resulting collapse mechanism is a symmetrical five-hinges mechanism which is depicted in Figure 6(b). The collapse load multiplier is $\lambda = 1.43$. In order to evaluate the effect of the limited compressive strength of masonry on the load capacity of the structure the same limit analysis has been carried out, allowing for a masonry compressive strength equal to 2.4 MPa, as indicated in Table 2 and as prescribed by the explicative circular [50] related to the Italian Building Code [51], following the algorithm described in Section 4. In this case the collapse load multiplier drops to $\lambda = 0.86$. As it has been explained in the previous Section it is also possible to account for the effect of FRP reinforcement. Indeed, during the seismic retrofit intervention a 200 mm wide strip of carbon fiber tissue (MapeWrap C Uni-AX produced by MAPEI) was applied to the extrados of the vault. This tissue has thickness of 0.2 mm, Young's elastic modulus of 230 GPa (for tensile stress only) and ultimate strain of 2%. FRP delamination force has been calculated by following the Italian FRP Design Guidelines [49]. By performing a limit analysis of the FRP reinforced arch, without taking into account the effect of limited compressive strength of masonry, the collapse load multiplier results $\lambda = 5.94$. In Figure 6(c) the symmetric five hinges collapse mechanism is shown: in this case the mechanism which develops only after FRP delamination has occurred at both sides of the arch. On the other hand, when the effect of finite compressive masonry strength is considered and coupled to the FRP reinforcement, the collapse load multiplier drops to $\lambda = 3.44$. Finally, an analysis of the original arch without reinforcement has been considered by accounting for possible sliding of masonry blocks as explained in Section 4. Therefore, after performing this limit analysis it can be observed that adopting a friction coefficient $\mu = 0.3$, as it is widely suggested in literature (see e.g. [53]), the original solution does not change: collapse still occurs by formation of a five hinges mechanism and the collapse multiplier is still $\lambda = 1.43$. Besides, if the friction coefficient is reduced to $\mu = 0.275$ it is observed that collapse mechanism modifies since sliding occurs at the arch imposts. In this last case the collapse multiplier is $\lambda = 1.02$ and the corresponding collapse mechanism and collapsed thrust line at collapse are shown in Figure 6(d).

6. Conclusions

This work introduced a new simple fully CAD-integrated approach to the analysis of masonry arches addressed to professionals in the field of structural rehabilitation of historical masonry constructions which cannot or do not want to get involved into more advanced computational tools. In particular, the proposed software provides a simple instrument for the accurate evaluation of the load bearing capacity of masonry arches. Furthermore, the open source computational tool ArchNURBS, which has been implemented in MATLAB[®], is freely available online (<http://...>)¹.

The new tool is based on NURBS description of the shape of the arch, which is designed in a CAD environment starting from a surveying data. A preliminary isogeometric finite element elastic analysis and a rigid-blocks limit anal-

¹ Authors: to be added before print



Figure 5: (a) External view and (b) first story masonry groin vault of *Torre Fornasini* (Poggio Renatico, Ferrara, Italy).

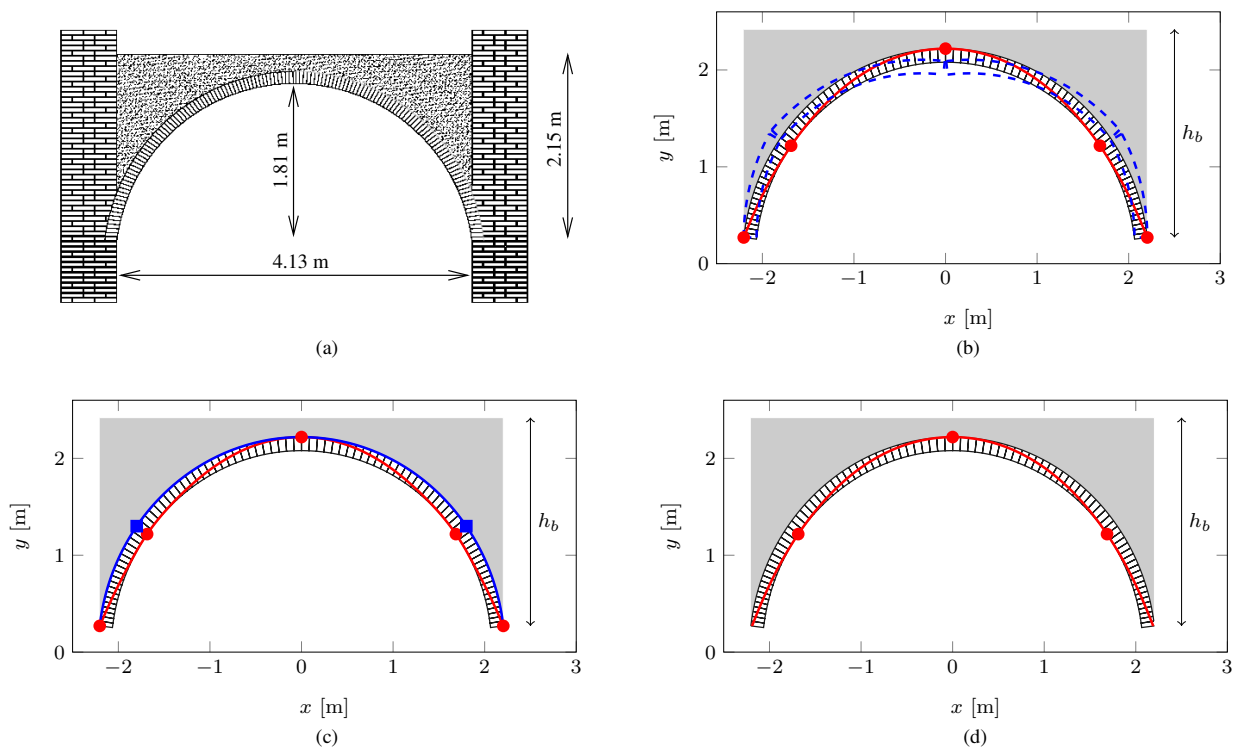


Figure 6: A masonry arch from *Torre Fornasini* in Poggio Renatico, (Ferrara, Italy) and represented in (a) has been examined. The thrust line (solid red line) and the position of the hinges (red circles) at collapse are illustrated in (b). Moreover, the solution of the limit analysis has been studied by considering (c) the FRP reinforcement indicated with a solid blue line (blue solid squares denote the FRP delamination points) and (d) sliding between blocks (with $\mu = 0.275$).

ysis of the masonry structure are possible. Furthermore, limited compressive strength for masonry, sliding between
355 blocks and presence of FRP reinforcement can be dealt with.

Some relevant examples of rigid-blocks limit analysis of masonry arches obtained with ArchNURBS have been
presented. Future research directions include a more sophisticated treatment of the problem of friction between
blocks and the adoption of a more advanced model for the backfill. Finally, an extension of the tool to the analysis of
three-dimensional masonry structures and in particular vaulted masonry systems will be developed.

360 Acknowledgements

The financial support of RAS, the Autonomous Region of Sardinia, under grant number F71J09999350002-CRP1.475
(Legge Regionale 7/2007, bando 2008, Progetto MISC: *Metodi Isogeometrici per Strutture Curve*) is gratefully ac-
knowledged by the second and by the fourth author. The researchers of the University of Ferrara gratefully acknowl-
edge the financial support of ReLUI3 program.

365 References

References

- [1] P. Roca, M. Cervera, G. Gariup and L. Pelà . Structural analysis of masonry historical constructions. *Engineering Structures* 2007;17:299–325.
- [2] A. Tralli, C. Alessandri and G. Milani . Computational methods for masonry vaults: a review of recent results. to appear on *The Open Journal of Civil Engineering* 2014;.
- 370 [3] LimitState Ltd. 2007 . Ring 3.0 Software. 2007. URL: <http://www.limitstate.it/ring>.
- [4] P. Gelfi . Arco 2008. 2008. URL: http://dicata.ing.unibs.it/gelfi/software/programmi_studenti.html.
- [5] AEDES Software per Ingegneria Civile . SAV. 2014. URL: <http://www.aedes.it>.
- [6] L. Piegl and W. Tiller . The NURBS book. 2nd ed.; Berlin: Springer Verlag; 1997.
- [7] T. J. R. Hughes, J. A. Cottrell and Y. Bazilevs . Isogeometric analysis: CAD, finite elements, NURBS, exact geometry and mesh refinement.
375 *Computer Methods in Applied Mechanics and Engineering* 2005;194:4135–95.
- [8] P. M. Prenter . Splines and variational methods. New York: Wiley; 1975.
- [9] C. de Boor . A practical guide to splines. 1st ed.; New York: Springer Verlag; 1978.
- [10] A. Benedetti and A. Tralli . A new hybrid F.E. model for Arbitrarily curved beam. I — Linear analysis. *Computers and Structures*
1989;33(6):1437–49.
- 380 [11] C. Gontier and C. Vollmer . A large displacement analysis of a beam using a CAD geometric definition. *Computers and Structures* 1995;57.
- [12] Y. Bazilevs, V. M. Calo, Y. Zhang and T.J.R. Hughes . Isogeometric fluid-structure interaction analysis with applications to arterial blood
flow. *Computational Mechanics* 2006;38:310–22.
- [13] J. A. Cottrell, T.J.R. Hughes and Y. Bazilevs . *Isogeometric Analysis: Toward Integration of CAD and FEA*. New York: Wiley; 2009.
- [14] D.J. Benson, Y. Bazilevs, M.C. Hsu and T.J.R. Hughes . Isogeometric shell analysis: the Reissner-Mindlin shell. *Computer Methods in*
385 *Applied Mechanics and Engineering* 2010;199:276–89.
- [15] F. Auricchio, L. Beirão da Veiga, T. J. R. Hughes, A. Reali and G. Sangalli . Isogeometric collocation for elastostatics and explicit dynamics.
Computer Methods in Applied Mechanics and Engineering 2012;249–252:2–14.
- [16] S. Huerta . Mechanics of masonry vaults: the equilibrium approach. In: R.B. Lourenço and P. Roca , editor. *Historical constructions*.
Guimarães; 2001, p. 47–69.
- 390 [17] M. Como . *Statics of historic masonry constructions*. Berlin-Heidelberg: Springer Verlag; 2013.

Please cite this document as: A. Chiozzi, M. Malagú, A. Tralli, A. Cazzani, “ArchNURBS: NURBS-Based Tool for the Structural Safety Assessment of Masonry Arches in MATLAB” *Journal of Computing in Civil Engineering*, 2016, 30(2): 04015010-1–04015010-11 DOI:10.1061/(ASCE)CP.1943-5487.0000481

- [18] J. Heyman . The stone skeleton. *International Journal of Solids and Structures* 1966;2:249–79.
- [19] J. Heyman . The masonry arch. Chichester: Ellis Horwood; 1992.
- [20] A. J. S. Pippard . An experimental study of the voussoir arch. *Proceedings ICE* 1939;10:383–404.
- [21] A. Kooharian . Limit analysis of voussoir (segmental) and concrete arches. *Journal American Concrete Institute* 1952;23:317–28.
- 395 [22] M. A. Crisfield . Non-linear finite element analysis of solids and structures; vol. 1 and 2. 2nd ed.; Wiley; 1997.
- [23] P. A. Cundall and O. D. L. Strack . A discrete numerical model for granular assemblies. *Geotechnique* 1979;29:47–65.
- [24] A. Munjiza . The combined finite-discrete element method. 1st ed.; Wiley; 2004.
- [25] R. K. A. Livesley . A computational model for the limit analysis of three-dimensional masonry structures. *Meccanica* 1992;27:161–72.
- [26] A. Orduna and P. Lourenço . Cap model for limit analysis and strengthening of masonry structures. *ASCE Journal of Structural Engineering*
400 2003;129:1367–75.
- [27] S. Briccoli Bati, M. Fagone and T. Rotunno . Lower bound limit analysis of masonry arches with CFRP Reinforcements: a numerical method. *Journal of Composites for Construction* 2013;17:543–53.
- [28] A. Caporale, L. Feo, D. Hui and R. Luciano . Debonding of FRP in multi-span masonry arch structures via limit analysis. *Composite Structures* 2014;108:856–65.
- 405 [29] I. Basilio, R. Fedele, P.B. Lourenço and G. Milani . Assessment of curved FRP-reinforced masonry prisms: experiments and modeling. *Construction and Building Materials* 2014;51:492–505.
- [30] M. G. Cox . The numerical evaluation of B-splines. *Journal of the Institute of Mathematics and its Applications* 1972;10:134–49.
- [31] G. Farin . *Curves and Surfaces for CAGD: A Practical Guide*. 5th ed.; San Francisco: Morgan Kaufmann Publishers; 2002.
- [32] P. J. Hartley and C. J. Judd . Parametrization and shape of B-spline curves for CAD. *Computer-Aided Design* 1980;12:235–8.
- 410 [33] E. T. Y. Lee . Choosing nodes in parametric curve interpolation. *Computer-Aided Design* 1989;21:363–70.
- [34] B. Sarkar and C-H. Menq . Smooth-surface approximation and reverse engineering. *Computer-Aided Design* 1991;23:623–8.
- [35] AUTODESK MAYA 8.5 - NURBS modeling. Autodesk; 2007.
- [36] A. Cazzani, M. Malagù and E. Turco . Isogeometric analysis of plane curved beams. *Mathematics and Mechanics of Solids*
2014; <http://dx.doi.org/10.1177/1081286514531265>.
- 415 [37] L. Greco and M. Cuomo . B-Spline interpolation of Kirchhoff-Love space rods. *Computer Methods in Applied Mechanics and Engineering*
2013;256:251–69.
- [38] L. Greco and M. Cuomo . An implicit G1 multi patch B-spline interpolation for Kirchhoff-Love space rods. *Computer Methods in Applied Mechanics and Engineering* 2014;269:173–97.
- [39] M. Lipshultz . *Theory and problems of differential geometry*. McGraw-Hill; 1969.
- 420 [40] J. A. Cottrel, T. J. R. Hughes and A. Reali . Studied of refinement and continuity in isogeometric structural analysis. *Computer Methods in Applied Mechanics and Engineering* 2007;196:4160–83.
- [41] A. Charnes and H. J. Greenberg . Plastic collapse and linear programming. *Bulletin of the American Mathematical Society* 1951;57:480–5.
- [42] R. K. A. Livesley . Limit analysis of structures formed from rigid blocks. *International Journal for Numerical Methods in Engineering*
1978;12:1853–71.
- 425 [43] J. M. Delbecq . Analyse de la stabilit  des vo tes en ma onnerie et en b ton non arm  par le calcul   la rupture. Document interne SETRA 1980;.
- [44] T. E. Boothby . Stability of masonry piers and arches including sliding. *ASCE Journal of Engineering Mechanics* 1994;120:304–19.
- [45] M. Gilbert and C. Melbourne . Rigid-block analysis of masonry structures. *The structural engineer* 1994;72:356–61.
- [46] M. Gilbert . Limit analysis applied to masonry arch bridges: state-of-the-art and recent developments. *Proc 5th International Conference on*
430 *Arch Bridges* 2007;:13–28.
- [47] J. Heyman . The safety of masonry arches. *International Journal of Mechanical Sciences* 1969;11:363–85.
- [48] LimitState Ltd . *Ring User Manual Version 3.0*. Sheffield UK; 2011.
- [49] Consiglio Nazionale delle Ricerche . DT200 R2013 - Istruzioni per la Progettazione, l'Esecuzione ed il Controllo di Interventi di Consolida-

- mento Statico mediante l'utilizzo di Compositi Fibrorinforzati. 2013.
- 435 [50] Circolare n. 617 02/02/2009 . Istruzioni per l'applicazione delle nuove Norme Tecniche per le Costruzioni di cui al decreto ministeriale 14 gennaio 2008. Gazzetta Ufficiale della Repubblica Italiana; 2009.
- [51] D.M. 14/01/2008 . Norme Tecniche per le Costruzioni. Gazzetta Ufficiale della Repubblica Italiana; 2008.
- [52] G. Milani, S. Marzocchi, F. Minghini and A. Tralli . Seismic assessment of a masonry tower in the region stricken by the 20-29 May 2012 Emilia-Romagna, Italy, earthquake. Proceedings of the 9th International Masonry Conference 2014;.
- 440 [53] G. Vasconcelos and P. B. Lourenço . Assessment of the in-plane shear strength of stone masonry walls by simplified models. Proceedings of the 5th International Conference Structural Analysis of Historical Constructions 2006;.